Sox2 expression in Schwann cells inhibits myelination in vivo and induces influx of macrophages to the nerve.

Running title: Sox2 inhibits PNS myelination

Sheridan L. Roberts[1]*, Xin-peng Dun[1]*, Robin D. S. Doddrell[1],Thomas Mindos[1], Louisa K. Drake[2], Mark W. Onaitis[3], Francesca Florio[4], Angelo Quattrini[4], Maurizio D'Antonio[4] and David B. Parkinson[1].

1. Plymouth University Peninsula Schools of Medicine and Dentistry, John Bull Building, Plymouth Science Park, Plymouth, PL6 8BU, UK.
2. University of Bath, Bath BA2 7AY, England, UK.
3. Dept. of Thoracic Surgery, University of California, San Diego, USA.
4. Division of Genetics and Cell Biology, and 4. Division of Neuroscience, San Raffaele Scientific Institute, DIBIT, 20132 Milan, Italy.

*S. R. and X-P.D are joint first authors.

Corresponding author: Prof. David Parkinson

e-mail: david.parkinson@plymouth.ac.uk

Telephone: +44 1752 431037

Fax: +44 1752 517846

Keywords: Schwann cell, myelination, Sox2, development, repair, peripheral nervous system.

Summary statement:

We show that, in vivo, the Sox2 transcription factor is a potent inhibitor of Schwann cell myelination, promoting both Schwann cell proliferation and macrophage infiltration in peripheral nerve.

Abstract

Correct myelination is crucial for the function of the peripheral nervous system. Both positive and negative regulators within the axon and Schwann cell function to ensure the correct onset and progression of myelination during both development and following peripheral nerve injury and repair. The Sox2 transcription factor is well known for its roles in the development and maintenance of progenitor and stem cell populations, but has also been proposed in vitro as a negative regulator of myelination in Schwann cells. We wished to test fully whether Sox2 regulates myelination in vivo and show here that sustained Sox2 expression in vivo blocks myelination in the peripheral nerves and maintains Schwann cells in a proliferative non-differentiated state, associated also with increased inflammation within the nerve. The plasticity of Schwann cells allows them to re-myelinate regenerated axons following injury and we show that re-myelination is also blocked by Sox2 expression in Schwann cells. These findings identify Sox2 as a physiological regulator of Schwann cell myelination in vivo and its potential to play a role in disorders of myelination in the peripheral nervous system.

Introduction

Schwann cells (SC) are the myelinating glia of the peripheral nervous system (PNS), they myelinate large diameter axons and provide trophic support for both motor and sensory axons. The transcriptional programmes driving both myelination and the dedifferentiation of SCs following injury have been partially characterised and many positive regulators such as Krox20 (Egr2), Oct6 (SCIP or Tst1), Sox10 and NFATc4 have been identified by both *in vitro* and *in vivo* analysis. However there is still little data on potential negative regulators of myelination *in vivo* that play roles in both the correctly timed onset of myelination and possibly in the pathology of demyelinating neuropathies of the PNS (Topilko et al., 1994, Svaren and Meijer, 2008, Jaegle et al., 1996, Finzsch et al., 2010, Kao et al., 2009, Jessen and Mirsky, 2008).

While the transcription factors Pax3, cJun and Sox2, activation of the Notch pathway, as well as signalling through the ERK1/2 and p38 mitogen activated protein (MAP) kinases, have been shown to inhibit myelination of SCs *in vitro*, there is only direct genetic evidence for Notch signalling, ERK1/2 and p38 activation regulating these processes *in vivo* (Yang et al., 2012, Le et al., 2005b, Parkinson et al., 2008b, Harrisingh et al., 2004b, Woodhoo et al., 2009b, Doddrell et al., 2012, Jessen and Mirsky, 2008, Napoli et al., 2012, Ishii et al., 2016, Ishii et al., 2013, Roberts et al., 2016).

The high mobility group (HMG) domain transcription factor Sox2 has been shown *in vitro*, using SC/dorsal root ganglion (SC/DRG) co-cultures and adenoviral over-expression of Sox2 in SCs, to inhibit the induction of Krox20 and myelination of axons (Le et al., 2005a), but a demonstration of the potential inhibitory role of Sox2 *in vivo* within the intact peripheral nerve has not yet been provided.

In order to test the role of Sox2 *in vivo*, we have made use of a conditional Sox2IRESGFP allele (Lu et al., 2010), which is activated in a cell-specific manner by crossing with the SC-specific P0-CRE line, and have tested the effects of ongoing Sox2 expression upon PNS myelination and repair. These experiments show, for the first time, that Sox2 *in vivo* will suppress PNS myelination and re-myelination following injury. In addition, persistent Sox2 expression in the adult nerve is sufficient to induce SC proliferation and an ongoing inflammatory state within the intact peripheral nerve.

Materials and Methods

Reagents

Adenoviruses expressing Krox20/GFP, Sox2/GFP and GFP control were previously described (Le et al., 2005b, Nagarajan et al., 2001, Parkinson et al., 2004a, Parkinson et al., 2008b). Antibodies against Sox2 were from Novus Biological (NB 110-37235SS) for western blotting and Millipore (AB5603) for immunostaining. Antibodies against myelin basic protein (MBP) (sc-13912),β2A Tubulin (sc-134229) and alpha6 integrin (F6) were from Santa Cruz Biotechnology (Wembley, UK). Antibodies to N-Cadherin (610920), β-catenin (610163) and cJun (610327) were from Becton-Dickinson (Oxford, UK). Antibody to Ki67 (Ab15580) was from Abcam (Cambridge, UK) and Krox20 (PRB-236P) from Covance (Cambridge, UK). Antibody to Sox10 was from Abcam (Ab155279) and laminin alpha2 antibody (ALX-804-190) from Enzo (Exeter, UK) Antibodies against myelin protein zero (P_0) and periaxin were as described (Archelos et al., 1993, Gillespie et al., 1994). Biotinylated antibodies, Alexafluor fluorescently conjugated antibodies and fluorescently conjugated streptavidin were as previously described (Doddrell et al., 2013b).

Transgenic mice and genotyping

Transgenic mouse breeding and experiments were carried out according to Home Office regulations under the UK Animals (Scientific Procedures) Act 1986. Ethical approval for experiments was granted by Plymouth University Animal Welfare and Ethical Review Board. To identify effects of Sox2 over-expression in SCs *in vivo,* we crossed homozygous Rosa26R-Sox2IRESGFP mice (Lu et al., 2010) with P0-CRE (mP_0-TOTACRE) mice (Feltri et al., 1999). This generated heterozygous Rosa26 Sox2IRESGFP CRE positive (+) and CRE negative (-) offspring. Heterozygous

Rosa26 Sox2IRESGFP CRE^{+} animals were then backcrossed with homozygous Rosa26 Sox2IRESGFP CRE^{-} mice to generate heterozygous and homozygous Rosa26R-Sox2IRESGFP CRE^{-} and CRE^{+} mice. CRE+ animals carrying one copy of the Rosa26 Sox2IRESGFP transgene are referred to as $Sox2^{HetOE}$; CRE+ animals carrying two copies of the Rosa26 Sox2IRESGFP transgene as $Sox2^{HomoOE}$ mice. For analysis of both $Sox2^{HetOE}$ and $Sox2^{HomoOE}$ mice, age and sex-matched CRE- animals of the same Rosa26 Sox2IRESGFP transgene status are used as controls. For mouse genotyping, genomic DNA was extracted using the HotSHOT method and analysed as previously described (Lu et al., 2010, Feltri et al., 1999, Truett et al., 2000).

Nerve Injury

For nerve crush injury, the right sciatic nerve was compressed using a pair of round end forceps, as previously described (Dun and Parkinson, 2015). The left sciatic nerve was left uninjured. Mice were euthanized at the indicated time and both the uninjured contralateral and injured distal sciatic nerves collected for analysis.

Cell culture and adenoviral infection

Rat SCs were prepared from postnatal day 3 rats, as previously described (Brockes et al., 1979, Parkinson et al., 2001). SCs were infected with GFP/Krox-20 (GFP/K20) (Parkinson et al., 2004a, Nagarajan et al., 2001), control GFP or GFP/ Sox2 adenovirus (Le et al., 2005b) or both GFP/Sox2 and GFP/K20 (Sox2/K20) adenovirus for 24 hours (h) in defined medium (DM) (Jessen et al., 1994) then incubated for a further 24h in DM before fixing and immunolabelling.

Immunocytochemistry, immunohistochemistry and western blotting

SCs were cultured on poly L-lysine/laminin coated glass coverslips as previously described (Jessen et al., 1994). For immunohistochemical analysis of nerve sections, nerves were fixed in 4% w/v paraformaldehyde and embedded for cutting of cryosections. All staining, antibodies, counts and confocal and fluorescence microscopy were as previously described (Doddrell et al., 2013a, Parkinson et al., 2008a, Parkinson et al., 2003b). Anti-MBP (1:100) and anti-Ki67 (1:200) antibodies were diluted in antibody diluting solution (ADS) with 0.2% Triton X-100 and incubated overnight at 4ºC. For western blotting, nerve samples were lysed in SDS buffer and protein electrophoresed on SDS-polyacrylamide gels. (Doddrell et al., 2013b, Parkinson et al., 2004a, Parkinson et al., 2008b, Parkinson et al., 2003a). β2A Tubulin was used as loading control for western blots.

Transmission electron microscopy (TEM)

Nerves were fixed in 2.5% glutaraldehyde in 0.1M phosphate buffer pH 7.2, post-fixed in 1% osmium tetroxide, dehydrated and embedded in resin. Semi-thin sections were cut using a glass knife and stained with toluidine blue. Ultra-thin sections were cut and stained with uranyl acetate and lead citrate. Sections were photographed and examined using a JEOL 1200EX, or 1400 TEM microscope. For quantification of G ratio in intact and injured nerves, axon diameter and fibre (axon + myelin) diameter was measured from 200 axons from each animal using Image J, which allowed for myelin thickness and G-ratio calculation. For quantification of

numbers of myelinated/degenerated fibres per field, average counts were made from 5 separate fields from both P60 control and $Sox2^{HomoOE}$ nerves.

Functional testing

Motor capacity in 6 and 8 week old mice was assessed by rotarod analysis. Rotarod training and final testing was as previously described (Saporta et al., 2012b, Kuhn et al., 1995). For these tests, the rod accelerated from 2 to 30 rotations per minute over a time period of 250 seconds.

For measurements of nerve conduction velocity (NCV), sciatic nerves from P21 or P90 animals were dissected and placed into a perfusion chamber for 30-45 minutes before measurements were initiated. During this time the sciatic nerves were incubated at 37ºC, and perfused with artificial cerebrospinal fluid (aCSF) as previously described (Fern et al., 1998, Alix and Fern, 2009). The distal end of the sciatic nerve were positioned within an aCSF filled glass stimulating electrode and compound action potentials (CAP) induced as previously described (Alix and Fern, 2009). CAPs were recorded by the second recording aCSF filled glass electrode surrounding the proximal end of the sciatic nerve (Fern et al., 1998) and displayed using Signal software (Cambridge Electronic Design). NCVs were calculated using two parameters: (1) the length of the stimulated nerve, and (2) the time difference between the start of the stimulus artefact to the peak of the CAP.

Functional recovery was measured on mice following injury using the static sciatic index (SSI) measurement. Paw print measurements were taken using a video camera from each mouse before surgery (0 days) and up to 21 days following injury to calculate the SSI (Baptista et al., 2007).

Statistics

For all experiments n=3 unless otherwise stated. All graphs display the arithmetic mean with error bars representing one standard error of the mean. Statistical analysis was carried out using a student t-test and p-value used to denote significance. Significance was calculated between control and test groups and denoted on figures as: * $p< 0.05$, ** $p< 0.01$ and *** $p<0.005$.

Due to small sample sizes ($n<5$ for most comparisons), assumptions of how well normality and equal variances fit data could not be reliably assessed. Sample size was not predetermined by statistical methods and randomisation not applied. For functional testing by SSI, the evaluation was made by an individual blinded to the animal genotype. No samples or data were excluded from the analysis. The n number for each experiment is stated in the appropriate Figure legend.

Results

Sox2 blocks Krox20-driven expression of myelin-associated proteins.

The analysis of mice with a hypomorphic allele of Krox20/Egr2 ($Egr2^{Lo/Lo}$) showed both PNS hypomyelination and continued post-natal expression of the Sox2 transcription factor in SCs (Le et al., 2005a). This study also showed that high levels of Sox2 in SCs blocked the *in vitro* induction of Krox20 by cyclic AMP and myelination in SC/DRG co-cultures. Previous analysis of inhibitors of myelination, for example the cJun transcription factor, have shown that, cJun can both inhibit the induction of Krox20 in SCs as well as preventing the activity of exogenously expressed Krox20 to induce myelinating SC markers. In this way, cJun acts as an inhibitor of myelination both upstream and downstream of Krox20 function (Parkinson et al., 2004b). While Sox2 has been shown to block Krox20 induction in SCs by cyclic AMP (Le et al., 2005a) we tested whether maintained Sox2 can also inhibit the action of the pro-myelinating transcription factor Krox20 to induce myelinating SC markers (Parkinson et al., 2004b). In adenoviral co-infection experiments, as expected, Krox20 induced both the expression of myelin protein zero (P_0) and the myelinating cell marker periaxin in SCs (Parkinson et al., 2003b, Parkinson et al., 2004b). Co-expression of Sox2 with Krox20 in SCs showed that Sox2 strongly antagonised Krox20-induced expression of both P_0 and periaxin (Fig. 1 A-H, I), confirming, *in vitro*, that maintained Sox2 expression can block the myelination programme both upstream and downstream of Krox20 induction in SCs.

Sox2 expression inhibits myelination *in vivo*.

We next tested whether Sox2 can act as an inhibitor of myelination *in vivo* within the intact nerve. A conditional over-expressing allele for Sox2 (Sox2IRESGFP), inserted into the Rosa26 locus, has been previously described that upon CRE-mediated recombination will express both Sox2 and enhanced green fluorescent protein (GFP) (Lu et al., 2010). In order to drive SC-specific expression of Sox2, we used the well characterised mP_0TOTA-CRE (P0-CRE) line (Feltri et al., 1999) to remove the floxed 'stop-cassette' sequence and allow cell-specific expression of Sox2 and GFP in SCs. We have characterised nerves from transgenic CRE+ mice that have either one ($Sox2^{HetOE}$) or both ($Sox2^{HomoOE}$) recombinant Rosa26-Sox2IRESGFP alleles and the effects of Sox2 expression upon PNS myelination and repair.

We first analysed sciatic nerves of mice carrying one copy of the Sox2IRESGFP transgene. Rosa26 wild-type/Sox2IRESGFP/CRE+ mice ($Sox2^{HetOE}$) showed both Sox2 and GFP expression in the SCs of the nerve. Sox2 expression in control and $Sox2^{HetOE}$ nerves was confirmed by western blot and immunolabelling (Fig. 2I, J and Fig. S1 A-D). These nerves and controls were analysed at postnatal day (P) 7 and P21 time points by transmission electron microscopy (TEM) (Fig. 2A-D). While there is no apparent defect at this stage in axonal sorting, SCs appear to make a normal 1:1 relationship with the axons, there is a substantial reduction in myelin thickness at P7 (Fig. 2 B, E) and at P21 (Fig. 2 D, G), resulting in an increased average G-ratio (0.71±0.003) for $Sox2^{HetOE}$ compared to 0.68±0.002 for control at P21. Western blotting of sciatic nerve from control and $Sox2^{HetOE}$ at both P3 and P7 showed

decreases in Krox20 and the myelin proteins P_0 and myelin basic protein (MBP, Fig. 2I). We also observed significant increases in the numbers of un-myelinated axons at both P7 and P21 in $Sox2^{HetOE}$ nerves compared to controls (Fig. 2 F, H).

Analysing $Sox2^{HetOE}$ animals at later timepoints, we observed that the myelination in the PNS appeared to return to normal. At P60 there was no significant difference in G-ratio compared to control animals (0.65±0.02 for $Sox2^{HetOE}$ compared to 0.66±0.02 for controls), nerve morphology of $Sox2^{HetOE}$ nerves was completely normal at P60 (Fig. 3 L and Fig. S1 J-L) and electrophysiology of $Sox2^{HetOE}$ nerves showed no changes in nerve conduction velocity at P90 compared to control nerves (Fig. S1 I). We analysed expression of the Sox2IRESGFP transgene in these $Sox2^{HetOE}$ animals and found that the expression of both Sox2 and GFP was high at P7 but declined from P21 onwards and were both undetectable at later timepoints, either by western blot or by immunocytochemistry (Fig. 2 J and Fig. S1 A-H)). We were unable to discern why expression levels of Sox2 and GFP decline in these $Sox2^{HetOE}$ mice, but it does show that loss of Sox2 over-expression in a hypomyelinated nerve from P21 onwards will allow myelination to proceed and apparently complete normally by P60 in the mouse PNS.

Next, we performed crosses to generate animals carrying two copies of the Sox2IRESGFP transgene and examined whether in this case Sox2 expression persisted in the nerve in CRE+ ($Sox2^{HomoOE}$) animals and the effects of such expression. $Sox2^{HomoOE}$ animals showed a similar hypomyelinating phenotype with ongoing Sox2 expression at P7, P14 and P21 timepoints in CRE+ animals and Sox2

continued to be expressed up to P60, as measured by either immunolabelling or western blot (Fig. 3 A-H, K and data not shown).

P60 adult $Sox2^{HomoOE}$ animals were smaller in size compared to controls and showed a typical hindlimb clasping when lifted by the tail (Fig. 3 N-P), indicating a possible reduction of PNS myelination. TEM analysis of P60 $Sox2^{HomoOE}$ nerves showed hypomyelination within the adult nerve (Fig. 3 I, J), showing that ongoing Sox2 expression will effectively inhibit myelination even at this later timepoint *in vivo*. Immunocytochemistry and western blotting of $Sox2^{HomoOE}$ nerves at both P7 and P60 showed reduced levels of Krox20 and of the myelin proteins P_0 and MBP (Fig. 3 K and Fig. S2 A-F, I). Levels of the Sox10 transcription factor protein, a key driver of myelination (Finzsch et al., 2010, Frob et al., 2012) were unchanged at P7, but actually increased in $Sox2^{HomoOE}$ nerves at P60 (Fig. S2 G), presumably due to increased numbers of SCs within the nerve. (see below and Fig. 7). Corresponding to the reduction in myelin protein expression, a significant increase in the G-ratio and numbers of unmyelinated axons was observed in $Sox2^{HomoOE}$ nerves at P60 compared to control and $Sox2^{HetOE}$ animals (Fig. 3 L, M).

More detailed examination of P7 and P60 $Sox2^{HomoOE}$ nerves showed a number of additional effects of Sox2 expression upon nerve morphology. At P7, although SCs are making a 1:1 relationship with axons, there is a stalling of the ensheathment (Fig. 4 A, B). Also at this age, where myelination is observed, we see an apparent lack of compaction in the outer myelin membrane layers of the SCs (Fig. 4 D, E). At P60, semi-thin and cryostat sections of $Sox2^{HomoOE}$ nerves show reduced myelination, but also some evidence of both axonal loss and ongoing myelin breakdown (Fig. 4 F, G, Q-T). Additionally at P60 we saw highly disorganised Remak bundles within the

$Sox2^{HomoOE}$ nerves, with groups of small diameter axons not separated by SC cytoplasm, in contrast to control nerves, and observed SCs extending abnormal processes and engulfing collagen fibres (Fig. 4 H-L). An examination of basal lamina structure in P60 $Sox2^{HomoOE}$ nerves with α6 integrin and laminin α2 staining showed an abnormal and diffuse staining pattern in $Sox2^{HomoOE}$ nerves as compared to controls (Fig. 4 M-P).

Similar SC behaviour was observed using in vitro SC/DRG myelinating co-cultures with Sox2-overexpressing SCs; 21 days after ascorbic acid addition to trigger myelination, Sox2 overexpressing SCs did not associate correctly with axons, produced many cellular processes and produced very little myelin as compared to controls (Fig. S3).

Sox2 over-expression reduces nerve conduction velocity (NCV), motor function and sensory function.

Following on from the molecular characterisation of nerves over-expressing Sox2, we next compared the NCV in control and $Sox2^{HetOE}$ animals. Analysis of compound action potentials in revealed that $Sox2^{HetOE}$ nerves have significantly decreased NCVs compared to control nerves at P21 (Fig. 5 A; see Fig. S4C for original electrophysiological recordings), although this had corrected by P90 (Fig. S1 I), consistent with the normal myelination at this timepoint in these animals (Fig S1 J-L). Next, motor functional analysis was tested using a rotarod with an increasing speed and recording the latency to fall (Saporta et al., 2012b, Wrabetz et al., 2006). A significantly reduced latency was observed in $Sox2^{HomoOE}$ mice at both 6 weeks and 8 weeks of age. Although not significant, a slight reduction in latency was also observed in $Sox2^{HetOE}$ mice at 6 weeks and 8 weeks of age (Fig. 5 B, C).

Further analysis of sensory function was carried out using toe pinch (pressure) and Von Frey filament (light touch) testing. At 6 weeks of age, toe pinch testing showed a reduction in the ability of $Sox2^{HomoOE}$ mice to response to pressure stimuli, compared to control and $Sox2^{HetOE}$ mice (Fig. S4 A). In testing using Von Frey filaments, we found that $Sox2^{HomoOE}$ mice also had a significantly decreased ability to respond to light touch stimuli compared to control mice (Fig. S4 B).

Increased levels of immature SC markers N-Cadherin and cJun in adult $Sox2^{HomoOE}$ nerves.

N-cadherin is expressed in the developing nerve and declines during myelination with a reciprocal up-regulation of E-cadherin, but is re-expressed following nerve injury (Crawford et al., 2008, Wanner et al., 2006). Expression of Sox2 in SCs has been shown to drive re-localisation of N-cadherin, a cell surface adhesion molecule, and allow SC clustering in the nerve bridge following PNS injury (Parrinello et al., 2010a). Such clustering is effected by the formation of adherens junctions through a calcium-dependent homophilic cadherin-cadherin interaction between SCs (Wanner and Wood, 2002). Immunolabelling of P60 sciatic nerve sections showed a clear increase in N-cadherin levels in SCs from $Sox2^{HomoOE}$ nerves compared to controls with an apparent cell membrane localisation (Fig. 6 A-D). Western blotting confirmed an increase in N-cadherin levels in $Sox2^{HomoOE}$ nerves as well as increased levels of the cJun transcription factor, a marker of promyelinating SCs (Parkinson et al., 2004b) (Fig. 6 I, J).

β-catenin is a binding partner of N-Cadherin and has been shown to both co-localise at the SC-axon interface to regulate SC polarity (Lewallen et al., 2011) and to positively regulate SC proliferation in SC-DRG co-cultures (Gess et al., 2008). β-catenin immunolabelling showed slightly raised levels of expression in P60 $Sox2^{HomoOE}$ nerves *in vivo* (Fig. 6 E-I). Corresponding *in vitro* experiments with rat SCs showed that enforced Sox2 expression alters SC morphology (Fig. S5 A, B), localises both N-cadherin and β-catenin to the SC membrane in a calcium-dependent manner (Fig. S5 C-J) and increased the levels of both proteins (Fig. S5 K); interestingly, expression of a 4-hydroxytamoxifen-regulatable Sox2 ($Sox2\text{-}ER^{TM}$) protein in 3T3 fibroblasts was also sufficient to drive upregulation and membrane localisation of the N-Cadherin protein following tamoxifen addition in this heterologous cell type (Fig. S6 A-E).

SC proliferation is increased by Sox2 expression *in vivo*.

In $Sox2^{HomoOE}$ mice we saw increased numbers of SCs within the nerve at ages from P7 onwards (Fig. 7 G, H and Fig. S7 F-M). To identify whether Sox2 increased SC proliferation *in vivo,* we immunolabelled P7 and P60 nerve sections with Ki67. The number of GFP/Ki67 positive nuclei was significantly increased in $Sox2^{HomoOE}$ mice at both P7 and P60 (Fig. 7 A-F, I, J), however no significant increase in Ki67 staining or nuclei number was detected at time points as early as P3 (Fig. S7 A-E and data not shown).

Increased numbers of macrophages in uninjured Sox2-overexpressing nerves.

Having observed that increased Sox2 expression maintains SCs in a proliferative non-myelinating state in the adult nerve, and also some myelin breakdown and axonal degeneration, we next tested whether this was associated with any increase in macrophages and other immune cells within the intact nerve. By double labelling for Iba1 and F4/80, we checked macrophage numbers in P7, P21 and P60 control and $Sox2^{HomoOE}$ nerves and found a significant increase in the number of macrophages within these intact $Sox2^{HomoOE}$ nerves at both P21 and P60 (Fig. 8 A-G). An increase, although not significant, was also found in the numbers of CD3 positive T-cells in intact P60 $Sox2^{HomoOE}$ nerves compared to controls (Fig. S8).

Sox2 over-expression impairs SC remyelination and functional recovery following nerve injury.

Although Sox2 re-expression has been shown to drive cell sorting in the nerve bridge following transection injury (Parrinello et al., 2010b), it is not known how maintained Sox2 expression in SCs will affect nerve repair and regeneration in the distal nerve following a crush injury. Thus, we next investigated the effect of maintained Sox2 expression on SC re-myelination for up to 21 days post crush injury (21DPI). As $Sox2^{HomoOE}$ animals show profound hypomyelination even at P60 we used $Sox2^{HetOE}$ animals for these experiments. As described above, in $Sox2^{HetOE}$ mice, Sox2 and GFP expression begins to decline at P21 and myelination corrects with a normal

nerve morphology and G-ratios at P60 as well as an unchanged nerve conduction velocity at P90 in these animals (above and Fig. S1 I-L).

As we observe transgene expression of both Sox2 and GFP at early developmental timepoints in the $Sox2^{HetOE}$ animals, we hypothesized that following PNS injury the accompanying de-differentiation of SCs distal to the injury site may be sufficient to cause re-activation of transgenic Sox2 and GFP expression in the $Sox2^{HetOE}$ animals, allowing us to study effects of ongoing Sox2 expression in a repairing nerve. This idea was proved correct and western blot and immunolabelling showed higher levels of Sox2 induction in $Sox2^{HetOE}$ animals compared to controls at 7 days post-crush injury (DPI) and that Sox2 and GFP expression were maintained at 21 DPI in these animals compared to controls (Fig. 9 A-F and L, M). Using TEM, we evaluated SC re-myelination by analysing distal nerve sections from control and $Sox2^{HetOE}$ mice at 21DPI. $Sox2^{HetOE}$ sciatic nerves distal to the site of injury were hypomyelinated (Fig. 9 G, H), with a significantly increased average G-ratio of 0.86±0.028 compared to control nerves, which had an average G-ratio of 0.69±0.028 at this timepoint (Fig. 9 I; see Fig. S9 A for G-ratio scatter plot). A significant increase in the percentage of unmyelinated axons and decrease in P_0 protein expression were observed in $Sox2^{HetOE}$ mouse nerves at 21DPI (Fig. 9 J, M).

Whilst numbers of regenerated axons were apparently unchanged, as visualised by neurofilament staining, further analysis of regenerated nerves at 21DPI did show a significant increase of axonal diameter in the repaired nerves of $Sox2^{HetOE}$ animals as compared to controls (Fig. S9 B), as well as significantly increased numbers of macrophages still present within the nerve at this timepoint (Fig. S9 C-G). No

significant difference in macrophage numbers was observed between uninjured nerves from control and $Sox2^{HetOE}$ animals (Fig. S9 G).

Having observed that Sox2 over-expression post-injury leads to a marked reduction in SC re-myelination in $Sox2^{HetOE}$ mice following injury, we next tested the functional recovery of these animals. Tests of functional recovery using an SSI measurement showed that recovery in $Sox2^{HetOE}$ mice was significantly reduced up to 21DPI compared to control mice (Fig. 9 K). This experiment validated that in addition to impairing remyelination, prolonged Sox2 expression in SCs following injury also attenuates functional recovery in these animals.

We next quantified re-myelination by analysing myelin protein re-expression following sciatic nerve injury. Corresponding to the TEM analysis (Fig. 9 G, H), western blotting confirmed that continued expression of Sox2 in the SCs of $Sox2^{HetOE}$ nerves following injury reduced the re-expression of P_0 at 21 DPI in the distal nerve (Fig. 9 L, M). Analysis of SC proliferation in the $Sox2^{HetOE}$ mice at 21 DPI also showed an ongoing and significantly increased proliferation in the nerve even at this timepoint after injury (Fig. 9 N), once more showing the potential for Sox2 to maintain SCs in an undifferentiated and proliferative state *in vivo* within the nerve.

Discussion

Within SCs, the onset of myelination is controlled by a network of transcription factors that co-operate to ensure a timely and appropriate ensheathment and myelination of axons (Svaren and Meijer, 2008). Mutations in many of these factors, such as those in the zinc finger protein Krox20 (Egr2), cause hypomyelinating neuropathies in both human patients and rodent models (Funalot et al., 2012, Baloh et al., 2009, Desmazieres et al., 2008, Arthur-Farraj et al., 2006, Warner et al., 1999, Warner et al., 1998).

Although there are a number of positive transcriptional regulators of myelination in SCs such as Krox20, Sox10, NFATc4 and Oct6, an increasing number of negative regulators of myelination such as MAP kinase signalling through p38 and ERK1/2 pathways, Notch signalling and the transcription factors Pax3 and cJun have been shown to block the myelination of SCs (Doddrell et al., 2012, Harrisingh et al., 2004a, Woodhoo et al., 2009a, Napoli et al., 2012, Yang et al., 2012, Parkinson et al., 2004b, Parkinson et al., 2008a).

The initial description of Sox2 as an inhibitor of PNS myelination came from the finding that mice with a hypomorphic Krox20 (Egr2) allele ($Egr2^{Lo/Lo}$), and thus reduced Krox20 expression, showed hypomyelination and increased expression of Sox2 in SCs. Further experiments, which aimed to determine the function of Sox2 as a negative regulator of myelination have used a virally-mediated expression system *in vitro.* These experiments showed that over-expression of Sox2 *in vitro* prevents both the induction of myelinating SC markers such as Krox20 and P_0 and enhanced the proliferation of SCs to the mitogen neuregulin (Le et al., 2005b). Whilst

this gives a good indication of Sox2 function, however, as assays of myelination *in* vitro may not fully reflect the situation *in vivo* (Lewallen et al., 2011, Golan et al., 2013), thus the aim of this study was to fully characterise the effects of maintained Sox2 expression upon both myelination and functional repair within the intact nerves of the PNS *in vivo*. In addition, this in vivo approach allows us to measure effects of maintained Sox2 expression in SCs upon immune cell influx into the nerve, both following injury and in the intact nerve.

Our experiments show a strong inhibitory effect of Sox2 on the myelination programme of SCs at all timepoints examined. The expression of myelinating SC markers such as Krox20, myelin basic protein and P_0 are all reduced and morphological analysis shows a severe hypomyelination of post-natal nerves. Correspondingly, an analysis of SC-specific Sox2 nulls has shown a slight acceleration of early post-natal myelination (MDA and X-PD, unpublished observations), confirming the inhibitory role of Sox2 in controlling developmental myelination. However, in contrast to experiments with SC-specific cJun and p38alpha MAP kinase nulls (Parkinson et al., 2008a, Roberts et al., 2016), we do not observe a function for Sox2 in the down-regulation of myelin proteins following injury. Injury experiments in Sox2 null nerves showed a similar profile of myelin protein loss compared to controls (X-PD, unpublished observations). Thus the role of Sox2 appears to be more important in regulating the onset of myelination both during development and following injury rather than in the events of SC dedifferentiation following axotomy.

An analysis of other potential Sox2 targets showed, both *in vitro* and *in vivo,* that Sox2 decreased mRNA and protein levels of the nectin-like protein Necl4 (also

known as Cadm4) in SCs (Fig. S10). Inhibition of Necl4 function in SCs, either by shRNA knockdown or expression of a dominant negative form of the protein, prevents normal SC-axon interaction, Krox20 induction and myelination *in vitro* (Maurel et al., 2007, Golan et al., 2013, Spiegel et al., 2007), but loss of Necl4 *in vivo* is associated with focal hypermyelination and a phenotype resembling several CMT subtypes (Golan et al., 2013); it is therefore unclear at present what role, if any, decreased Necl4 levels may play in the phenotype we observe in our Sox2 over-expressing animals.

Over-expression of the mammalian Lin28 homologue B (Lin28B) RNA binding protein and reduction of levels of the let-7 family of microRNAs in SCs has been shown to inhibit peripheral nerve myelination in vivo (Gokbuget et al., 2015). As Sox2 has been shown to increase Lin28B levels in embryonic stem cells and neural progenitors (Cimadamore et al., 2013, Marson et al., 2008), we measured Lin28B protein levels in control and $Sox2^{HomoOE}$ nerves at P60. We do not detect Lin28B expression in either control or $Sox2^{HomoOE}$ adult nerve (Fig. S2 H), therefore seemingly eliminating the Lin28B/let-7 signalling axis as mediating the Sox2-induced hypomyelination.

It is still unclear as to why the expression of the Sox2IRESGFP transgene declines in the $Sox2^{HetOE}$ animals up to P21, as the construct is inserted into the Rosa26 locus and the construct also contains a synthetic cytomegalovirus early enhancer / chicken beta actin (CAG) promoter (Lu et al., 2010), but these issues of silencing of the transgene expression were not seen in the $Sox2^{HomoOE}$ animals, allowing us to monitor the effects of Sox2 expression up to P60 in these animals. Analysis of $Sox2^{HetOE}$ nerves up to P60 allowed us to measure the effects of the

removal of Sox2 over-expression in SCs from P21 onwards. In this case the nerves continued their myelination and by P60 they appeared normally myelinated with G-ratios similar to control nerves, once again underlining a remarkable ability of SCs within the nerve to resume and complete their myelination programme.

The normal myelination observed in P60 $Sox2^{HetOE}$ nerves and re-activation of Sox2 expression following injury in these animals also allowed us to confirm that Sox2 negatively regulates both developmental myelination and re-myelination following injury, in contrast to some regulators within SCs that have developmental or repair-specific functions (Arthur-Farraj et al., 2012, Fontana et al., 2012, Kim et al., 2000, Jessen and Mirsky, 2016, Mindos et al., 2017).

Whether negative regulators of myelination play roles in the pathology of human peripheral neuropathies or mouse models of these conditions has been recently examined. Increased expression of the cJun transcription factor in SCs has been observed in both patients with Charcot-Marie-Tooth (CMT) disease, chronic inflammatory demyelinating polyradiculopathy and mouse models of CMT (Saporta et al., 2012a, Hutton et al., 2011, Hantke et al., 2014, Klein et al., 2014), and although it has been suggested that abnormal expression of cJun may be involved in the pathology of the hypomyelination seen (Saporta et al., 2012a), recent work using the C3 mouse model of CMT1A showed that cJun expression was actually protective. Genetic removal of cJun in the C3 mouse, which models human CMT1A, led to a progressive loss of myelinated sensory axons and increasing sensory-motor loss (Hantke et al., 2014). Thus, as opposed to driving the neuropathy in these animals, raised expression of cJun in SCs is a protective mechanism to ameliorate the disease state. Recent reports have shown that levels of Sox2 mRNA are elevated in

in mouse models of CMT types 1A and 1B (D'Antonio et al., 2013, Giambonini-Brugnoli et al., 2005), but any potential roles for this increased expression are currently unknown.

The finding of increased macrophage numbers within both the intact $Sox2^{HomoOE}$ nerve at P60 and within the $Sox2^{HetOE}$ nerve following injury suggests a role for Sox2 in the control of macrophage entry to the nerve, although it is not clear whether this is a direct effect or is due to the lack of myelination or the apparent ongoing myelin breakdown and axonal loss seen in the adult P60 $Sox2^{HomoOE}$ nerves (Fig. 4 F, G).

In conclusion, we have identified that Sox2 acts as an *in vivo* inhibitor of the myelinating phenotype of SCs and have shown new roles for this protein in both controlling the proliferation of SCs and recruitment of macrophages to the nerve.

Acknowledgments.

This work was supported by a grant from the UK Wellcome Trust (Ref. 088228/Z/09/Z) to D.B.P. MD is supported by Fondazione Telethon (GGP14147) and the Italian Ministry of Health (GR-2011-02346791). We are grateful for excellent technical support from Mr Peter Bond, Mr Glenn Harper and Dr Roy Moate in the Plymouth University EM Centre and Ms Cinzia Ferri and Dr Mariacarla Panzeri at the ALEMBIC service at the San Raffaele for help with TEM sample processing and imaging. We thank Prof. Bob Fern, Dr Angelo de Rosa and Mr Sean Doyle (Plymouth University) for help with electrophysiology measurements. We thank also Profs Laura Feltri and Larry Wrabetz (University of New York at Buffalo, USA) for providing the mP_0-TOTACRE mice. We are grateful to Mr W. Woznica for excellent technical support with animal husbandry for the study.

Author Contributions: S.L.R., X-P.D., R.D.S., T.M., F.F., A.Q., L.K.D., M.D.A. and D.B.P. performed experiments and analysed data. M.W. provided transgenic mice and experimental guidance. D.B.P., S.L.R. and M.D.A. wrote and edited the manuscript.

Conflict of Interest.

The authors declare that they have no conflict of interest.

Figures and Figure legends:

Figure 1.

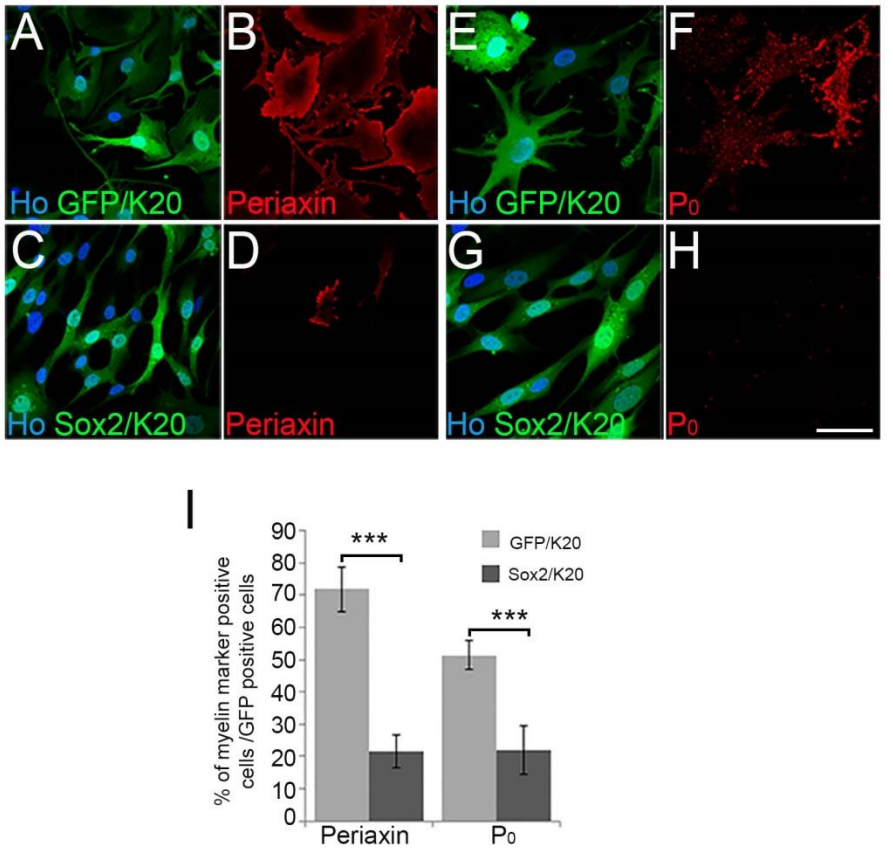

Figure 1: Sox2 antagonises Krox20 induced myelin protein expression *in vitro.*

A-H. Immunofluorescence of rat SCs infected with GFP/Krox20 (A, B, E, F) or Sox2/Krox20 (C, D, G, H) expressing adenovirus, showing inhibition of Krox20-driven periaxin (C, D) and P_0 expression (G, H) by Sox2. Hoechst stain (Ho) is used to reveal SC nuclei. Scale bars 20μm. M. Graph showing the percentage of periaxin and P_0 positive cells, in GFP/K20 and Sox2/K20 adenoviral infected SCs.

Figure 2.

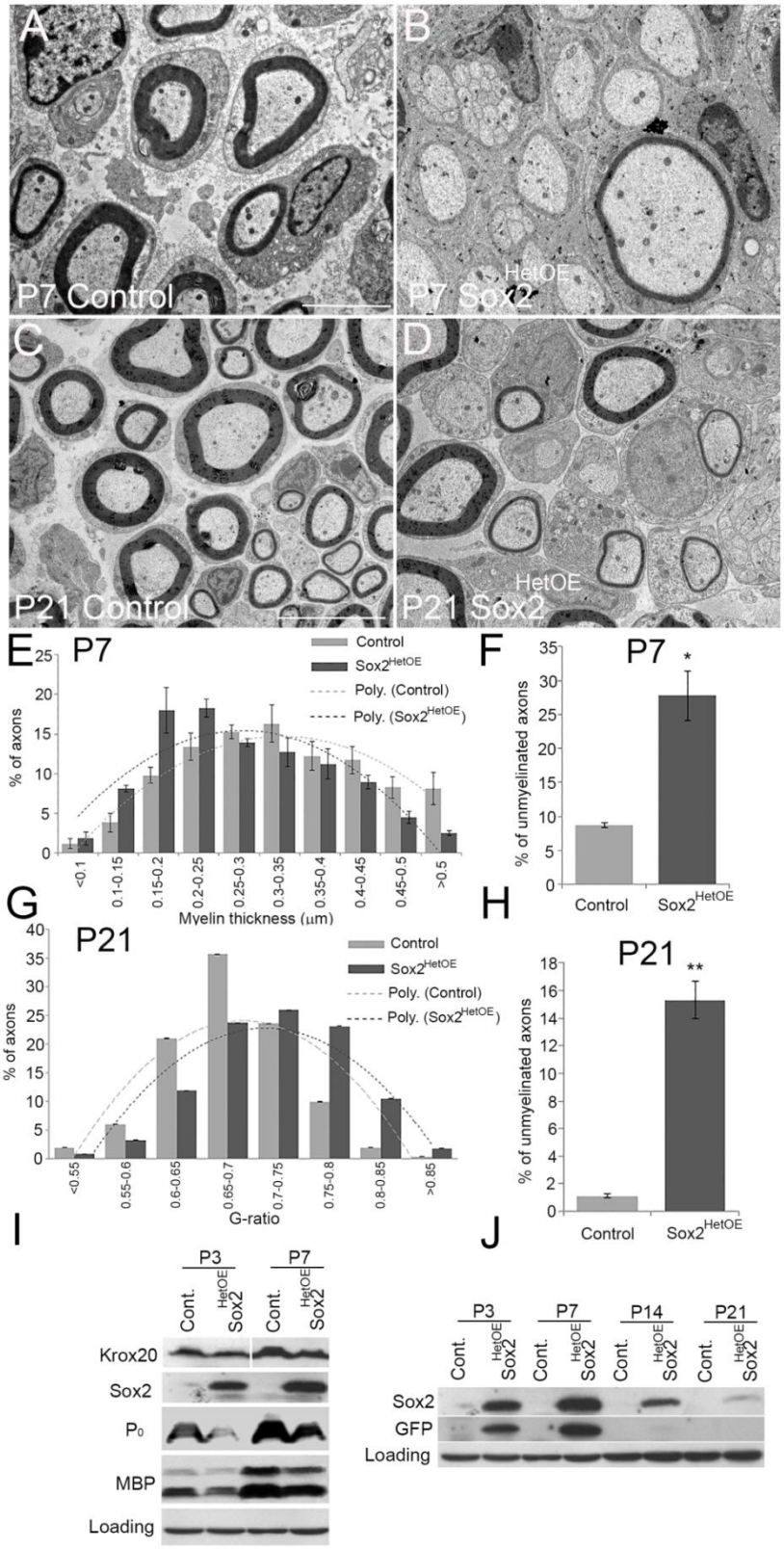
A
P7 Control
B
HetOE
P7 Sox2
C
P21 Control
D
HetOE
P21 Sox2
E
P7
Control
Sox2HetOE
Poly. (Control)
Poly. (Sox2HetOE)
% of axons
<0.1
0.1-0.15
0.15-0.2
0.2-0.25
0.25-0.3
0.3-0.35
0.35-0.4
0.4-0.45
0.45-0.5
>0.5
Myelin thickness (μm)
F
P7
*
% of unmyelinated axons
Control
Sox2HetOE
G
P21
Control
Sox2HetOE
Poly. (Control)
Poly. (Sox2HetOE)
% of axons
<0.55
0.55-0.6
0.6-0.65
0.65-0.7
0.7-0.75
0.75-0.8
0.8-0.85
>0.85
G-ratio
H
P21
**
% of unmyelinated axons
Control
Sox2HetOE
I
P3
P7
Cont.
HetOE Sox2
Krox20
Sox2
P0
MBP
Loading
J
P3
P7
P14
P21
Cont.
HetOE Sox2
Sox2
GFP
Loading

Figure 2: Inhibition of myelination in Sox2 over-expressing mice in vivo. A–D. TEM of sciatic nerves from control post-natal day (P) 7 control (A) and $Sox2^{HetOE}$ mice (B) and P21 control (C) and $Sox2^{HetOE}$ mice (D). Scale bar A-D 5 μm. E. Graph illustrating distribution of myelin thickness in control and $Sox2^{HetOE}$ mouse nerves. F. Graph showing a significant increase in the proportion of unmyelinated axons above 1μm diameter in the sciatic nerves of P7 $Sox2^{HetOE}$ mice compared to control mice. G. Graph showing the distribution of G-ratio of axons in P21 control and $Sox2^{HetOE}$ nerves. H. Graph showing a significant increase in the population of unmyelinated axons above 1μm diameter in the sciatic nerves of P21 $Sox2^{HetOE}$ mice compared to control mice. I. Western blots showing the reduction in Krox20, P_0 and myelin basic protein (MBP) proteins in P3 and P7 control and $Sox2^{HetOE}$ nerves. J. Western blots showing Sox2 and GFP expression in post-natal control and $Sox2^{HetOE}$ mice.

Figure 3.

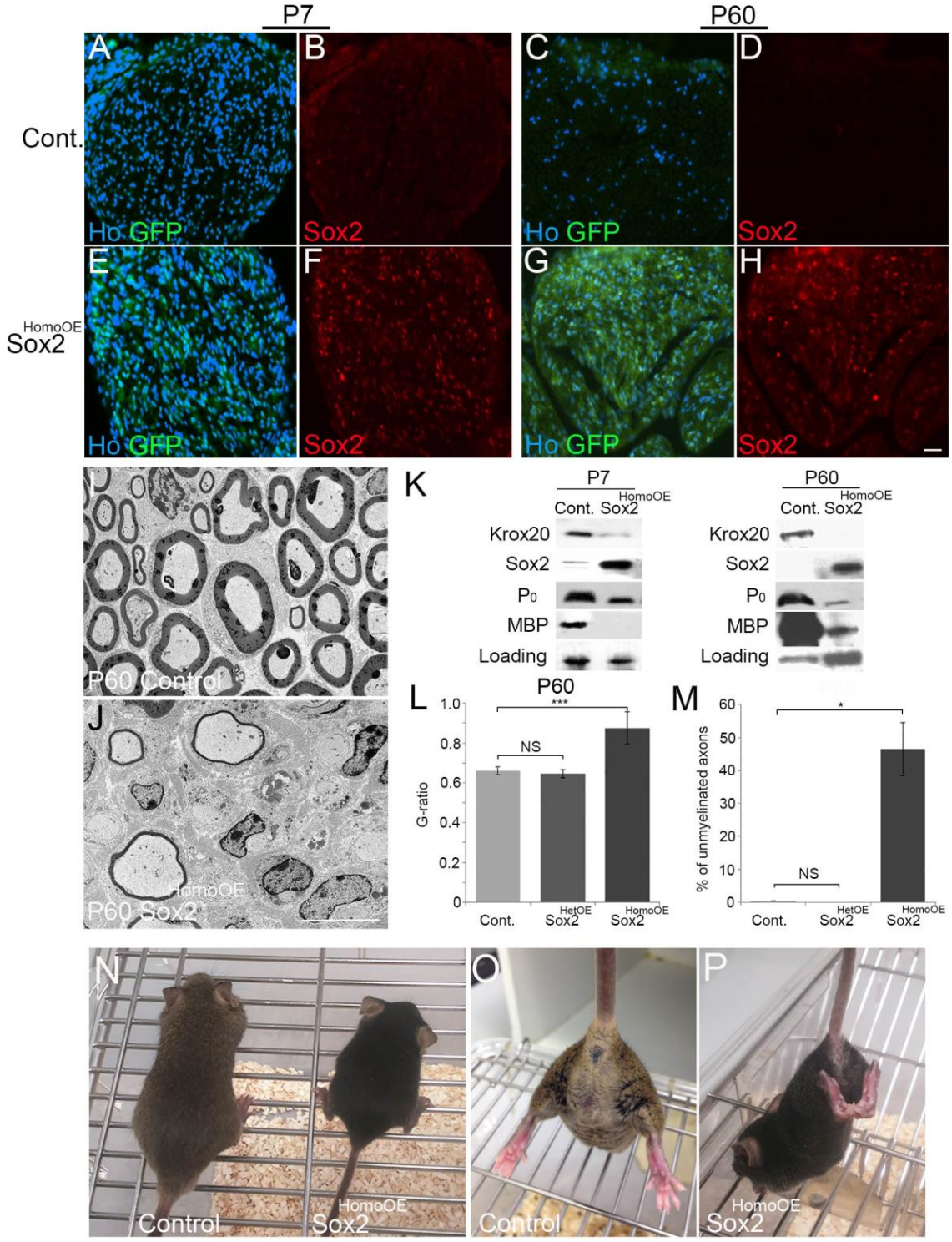

Figure 3: Analysis of Sox2 expression and myelination in Sox2^{HomoOE} mice carrying two copies of the Sox2IRESGFP transgene. A-H. Immunohistochemical analysis of sciatic nerves stained with Sox2 antibody demonstrates that control

nerves do not express GFP or Sox2 at P7 (A, B) or P60 (C, D), whereas $Sox2^{HomoOE}$ nerves have high levels of GFP and Sox2 expression at both P7 (E, F) and P60 (G, H) ages. Scale bars 40μm. I, J. TEM images of control (I) and $Sox2^{HomoOE}$ (J) nerves at P60. Scale Bar 5μm. K. Western blots of control and $Sox2^{HomoOE}$ nerves at P7 and P60 showing a reduction in Krox20, P_0 and MBP expression *in vivo* by Sox2 expression in SCs. L, M. G-ratio measurements (L) and numbers of unmyelinated axons above 1μm diameter (M) in control, $Sox2^{HetOE}$ and $Sox2^{HomoOE}$ nerves at P60. N. $Sox2^{HomoOE}$ mouse (black, on right side of picture) shows a reduced size at P60 compared to control animals. O, P. $Sox2^{HomoOE}$ animals (P) show hind limb clasping when lifted by the tail, characteristic of peripheral hypomyelination, compared to a control littermate (O).

Figure 4.

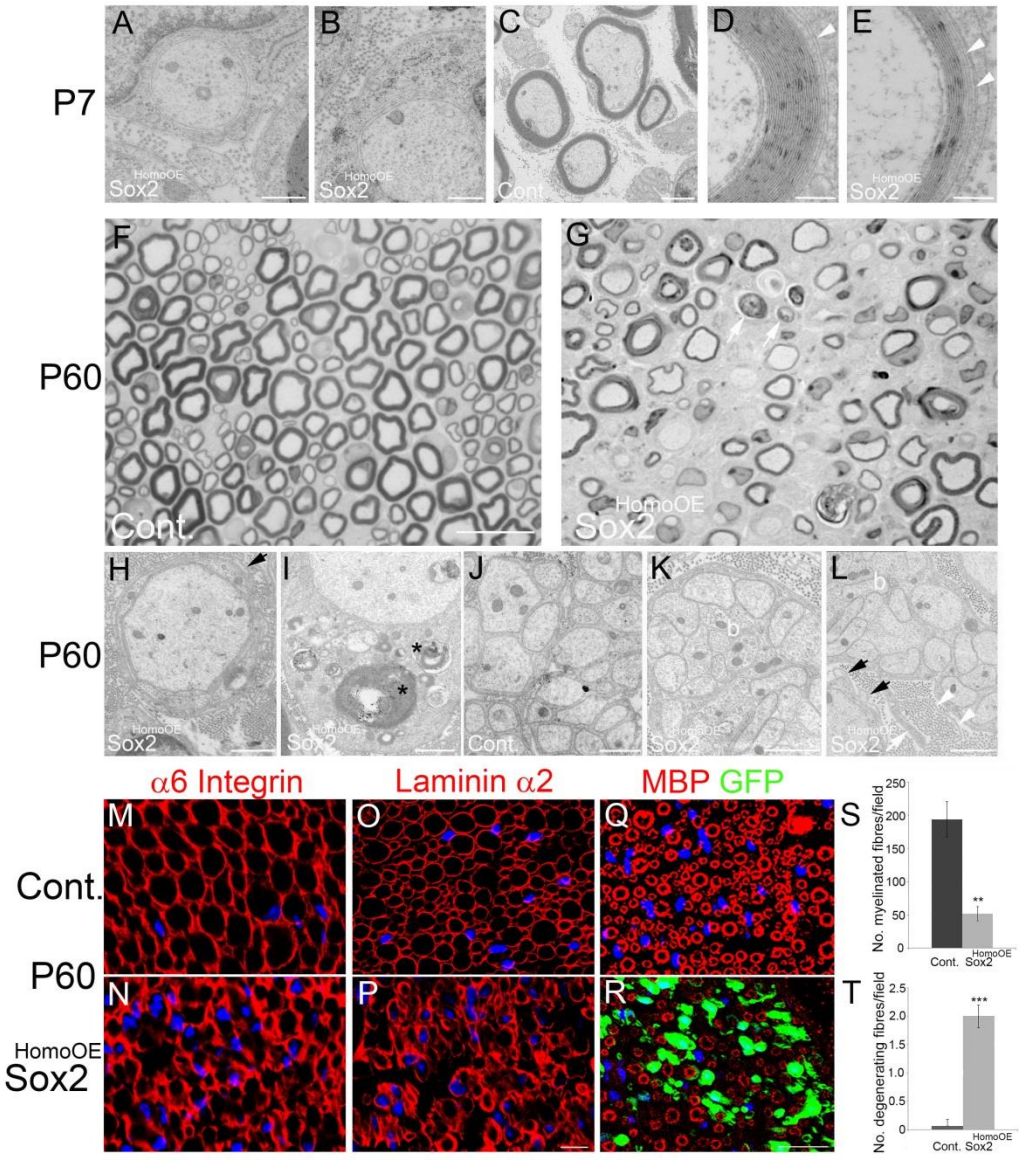

Figure 4: Morphology of P7 and P60 control and Sox2^{HomoOE} nerves. A-E. P7 sciatic nerves from control (C) and Sox2^{HomoOE} animals (A, B, D and E). Whereas in control nerves SCs have formed proper myelin (C), in Sox2^{HomoOE} nerves most SCs are stalled in the 1:1 stage (A, B). Where Sox2 over-expressing SCs do form myelin, they often show non-compaction of the outer myelin layers (white arrowheads in D and E). Scale bars A, B: 500nm; C: 2μm; D, E: 200nm. F, G. Semi-thin sections of P60 control (F) and Sox2^{HomoOE} (G) nerves; arrows in G indicate possible axonal loss

and demyelination. Scale bar 20μm. H-L. P60 control and Sox2^{HomoOE} nerves. At P60 most axons in Sox2^{HomoOE} nerves are amyelinated and are surrounded by redundant SC basal lamina (black arrows in H and L) and several SCs show myelin debris in the cytoplasm (asterisks in I). Remak bundles, that in control nerves show proper SC cytoplasm separating axons (J), show bundles of axons touching each other ('b' in K and L) and aberrant SC processes (white arrow in L) whose basal lamina forms collagen pockets (white arrowheads in L). Scale bars H-L 1μm. M-R P60 control and Sox2^{HomoOE} nerve sections immunolabelled with α6 integrin (M, N), laminin α2 (O, P) and myelin basic protein (MBP)/GFP (Q, R). Scale bars 5μm in M-P and 25 μm in Q, R. S, T. Quantification of numbers of myelinated (S) and degenerating (T) fibres per field in P60 control and Sox2^{HomoOE} nerves.

Figure 5.

Figure 5: Nerve conduction velocity and motor function is reduced in Sox2 over-expressing animals. A. Graph comparing the nerve conduction velocity (NCV) of sciatic nerves taken from control (n=11) and $Sox2^{HetOE}$ (n=13) mice at P21. B, C. Graph showing the reduction in latency to fall using rotarod testing of control, $Sox2^{HetOE}$ and $Sox2^{HomoOE}$ mice at 6 weeks (B) and 8 weeks (C) of age. 6 weeks control n=7, $Sox2^{HetOE}$ n=4 and $Sox2^{HomoOE}$ n=6; 8 weeks control n=4, $Sox2^{HetOE}$ n=4 and $Sox2^{HomoOE}$ n=6.

Figure 6.

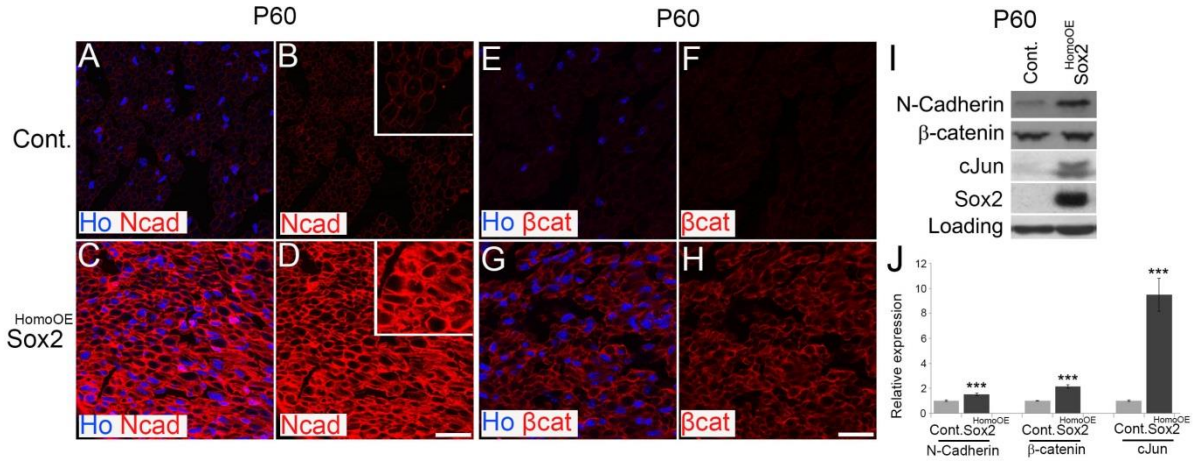

Figure 6: Expression and localisation of N-Cadherin and β-catenin in P60 Sox2^{HomoOE} nerves. A-H. Immunolabelling of sciatic nerve sections from P60 control (A, B, E and F) and Sox2^{HomoOE} (C, D, G and H) nerves showing localisation and levels of N-Cadherin (NCad, A-D) and β-catenin (βcat, E-H) in SCs. Sections are counterstained with Hoechst (Ho) to reveal nuclei. Scale bar 20μm. I. Western blot showing elevated levels of Sox2, N-Cadherin and cJun in P60 Sox2^{HomoOE} nerves as compared to controls. J. Quantification of western blots in panel I.

Figure 7.

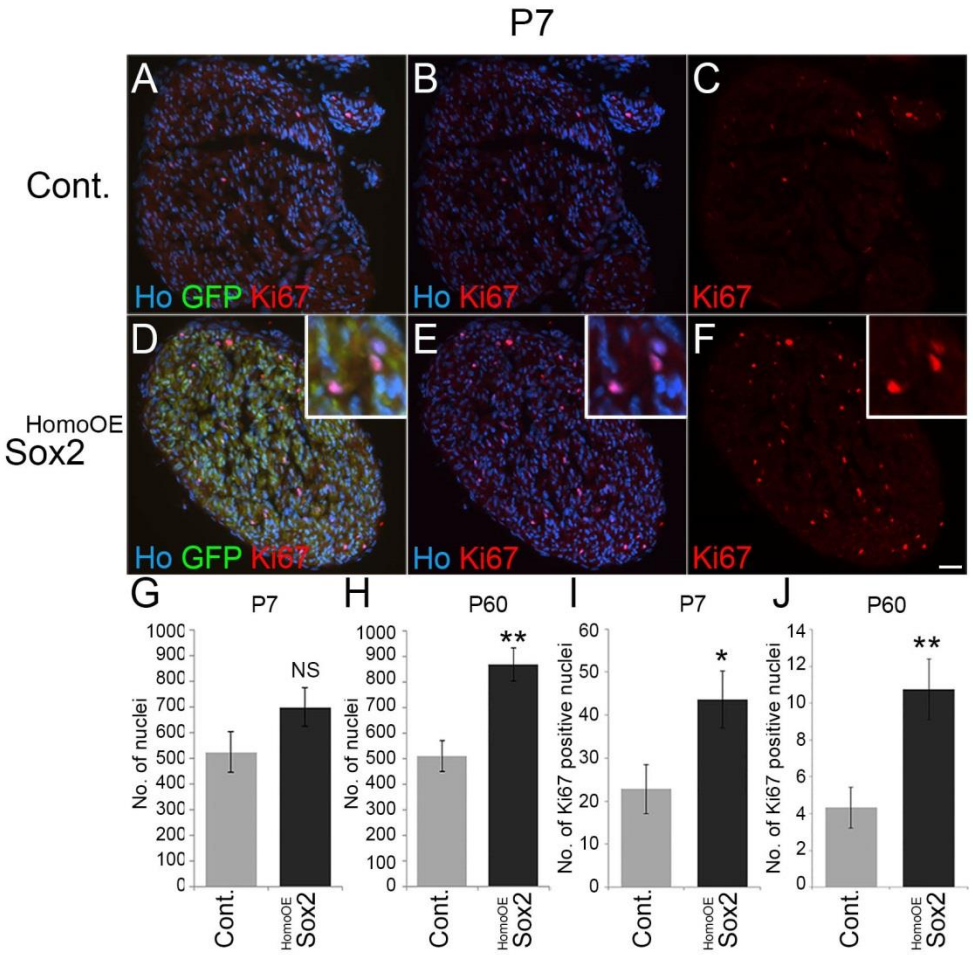

Figure 7: SC numbers and proliferation are increased in Sox2 over-expressing nerves. A-F. Sections of sciatic nerves taken from P7 control (A-C) and Sox2^{HomoOE} (D-F) mice were immunolabelled with antibodies against Ki67. Scale bar 40μm. Insets in panels D-F show higher magnification of Ki67/GFP positive SCs. G, H Graphs showing an increase in the number of SC nuclei in P7 (G) and P60 (H) Sox2^{HomoOE} sciatic nerves compared to controls. Numbers given are total nuclei per sciatic nerve transverse section. I, J Graph showing a significant increase in the number of GFP/Ki67 positive nuclei in P7 (I) and P60 (J) Sox2^{HomoOE} sciatic nerves compared to controls.

Figure 8.

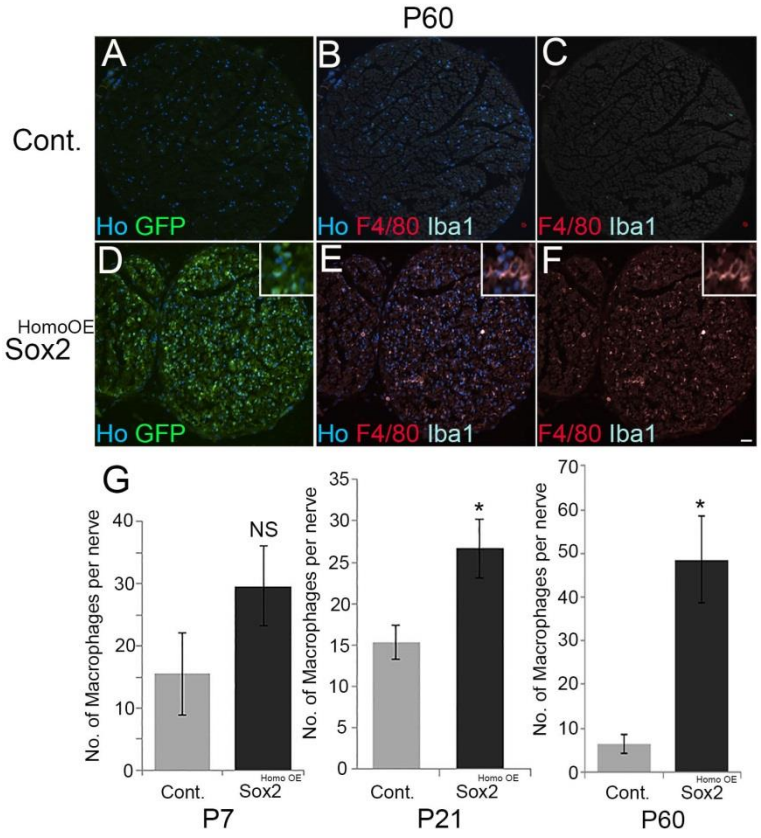

Figure 8: Increased numbers of macrophages in intact P60 Sox2^{HomoOE} sciatic nerves. Double immunolabelling of sciatic nerve sections from P60 control (A-C) and Sox2^{HomoOE} (D-F) sciatic nerves with F4/80 and Iba1 to identify macrophages. Scale bar 40μm. Insets in panels D-F show higher magnification of F4/80/Iba1 double-positive macrophages within the nerve. G. Graphs showing quantification of macrophage numbers at P7, P21 and P60; a significant increase in macrophage numbers is observed in both P21 and P60 Sox2^{HomoOE} nerves.

Figure 9.

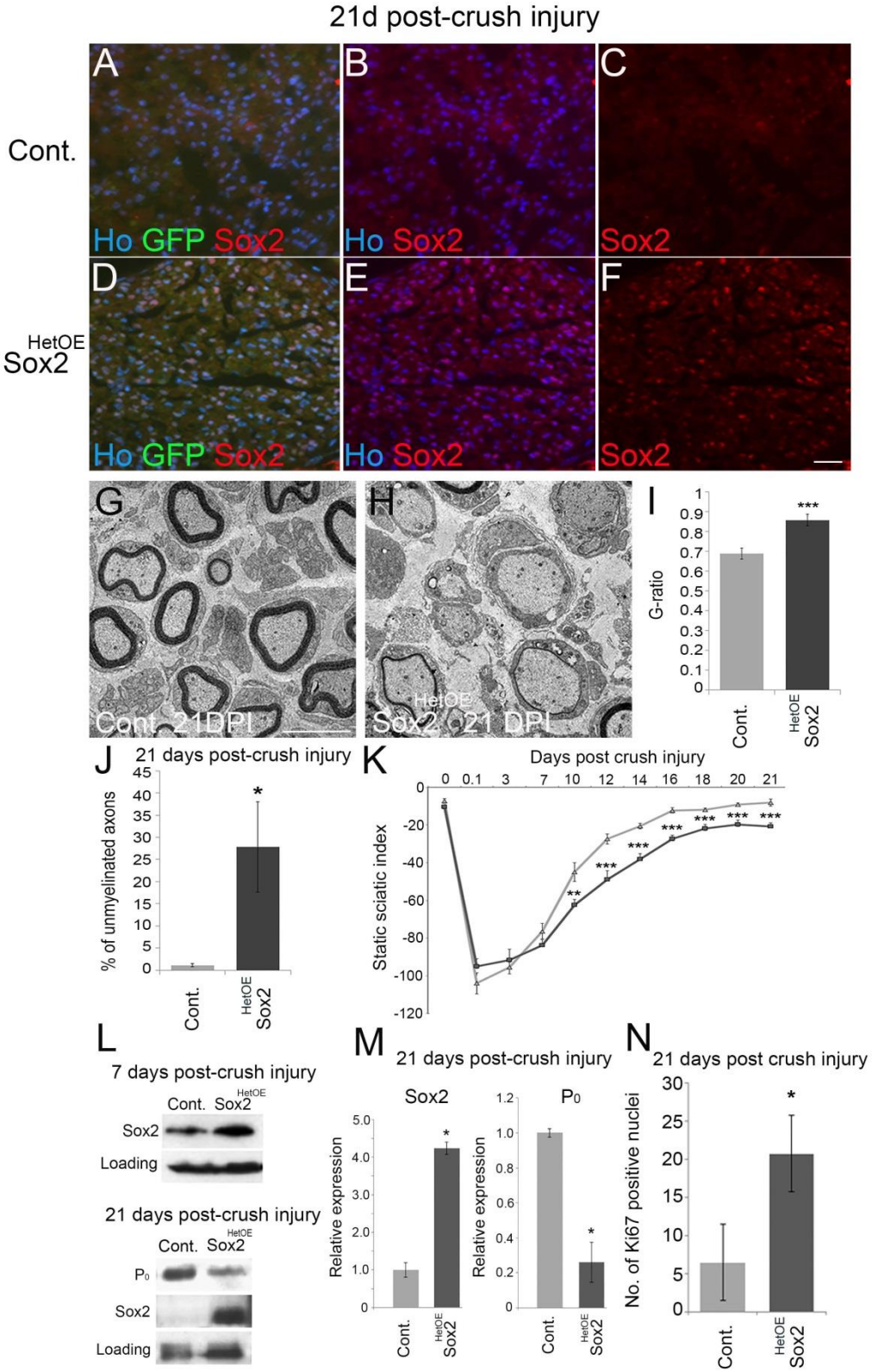
21d post-crush injury
Cont.
HetOE Sox2
A
B
C
D
E
F
Ho GFP Sox2
Ho Sox2
Sox2
G
H
I
Cont. 21DPI
HetOE Sox2 21 DPI
G-ratio
Cont.
HetOE Sox2
J
21 days post-crush injury
% of unmyelinated axons
K
Days post crush injury
Static sciatic index
L
7 days post-crush injury
Cont. Sox2 HetOE
Sox2
Loading
21 days post-crush injury
P0
M
21 days post-crush injury
Relative expression
N
21 days post crush injury
No. of Ki67 positive nuclei

Figure 9: Sustained Sox2 expression results in hypomyelination and reduced functional recovery following nerve injury. A-F Immunolabelling of distal sciatic nerves sections 21 days post-crush injury (DPI) with antibodies against Sox2, revealed that nerves from control animals no longer expressed Sox2 at this time point (A-C), whereas Sox2 (and GFP) levels remained elevated in the distal sciatic nerves of injured $Sox2^{HetOE}$ mice (D-F). Scale bar 40μm. G, H. TEM pictures of distal sciatic nerve sections at 21 DPI revealed that axons in control nerves are remyelinated (G), whereas few axons appear to be remyelinated in $Sox2^{HetOE}$ nerves (H). Scale bar 5μm I. G-ratio measurements revealed that $Sox2^{HetOE}$ sciatic nerves were significantly hypomyelinated compared to control nerves at 21 DPI. J. Graph showing a significant increase in the percentage of unmyelinated axons in $Sox2^{HetOE}$ nerves compared to control nerves at 21 DPI. K. Quantification of functional recovery by analysis of static sciatic index (SSI). Control n=5, $Sox2^{HetOE}$ n=7, L. Western blot showing high levels of Sox2 at 21DPI leads to a reduction in P_0 expression in $Sox2^{HetOE}$ mice. M. Quantification of western blots from panel L. N. Graph showing a significant increase in the number of Ki67 positive nuclei in distal $Sox2^{HetOE}$ sciatic nerves at 21 DPI compared to controls.

References:

ALIX, J. J. P. & FERN, R. 2009. Glutamate receptor-mediated ischemic injury of premyelinated central axons. *Annals of Neurology,* 66**,** 682-693.

ARCHELOS, J. J., ROGGENBUCK, K., SCHEIDER-SCHAULIES, J., LININGTON, C., TOYKA, K. V. & HARTUNG, H. P. 1993. Production and characterization of monoclonal antibodies to the extracellular domain of P0. *Journal of Neuroscience Research,* 35**,** 46-53.

ARTHUR-FARRAJ, P., LATOUCHE, M., WILTON, D. K., QUINTES, S., CHABROL, E., BANERJEE, A., WOODHOO, A., JENKINS, B., RAHMAN, M., TURMAINE, M., WICHER, G. K., MITTER, R., GREENSMITH, L., BEHRENS, A., RAIVICH, G., MIRSKY, R. & JESSEN, K. R. 2012. c-Jun reprograms Schwann cells of injured nerves to generate a repair cell essential for regeneration. *Neuron,* 75**,** 633-47.

ARTHUR-FARRAJ, P., MIRSKY, R., PARKINSON, D. B. & JESSEN, K. R. 2006. A double point mutation in the DNA-binding region of Egr2 switches its function from inhibition to induction of proliferation: A potential contribution to the development of congenital hypomyelinating neuropathy. *Neurobiol Dis,* 24**,** 159-69.

BALOH, R. H., STRICKLAND, A., RYU, E., LE, N., FAHRNER, T., YANG, M., NAGARAJAN, R. & MILBRANDT, J. 2009. Congenital hypomyelinating neuropathy with lethal conduction failure in mice carrying the Egr2 I268N mutation. *J Neurosci,* 29**,** 2312-21.

BAPTISTA, A. F., GOMES, J. R. D. S., OLIVEIRA, J. T., SANTOS, S. M. G., VANNIER-SANTOS, M. A. & MARTINEZ, A. M. B. 2007. A new approach to assess function after sciatic nerve lesion in the mouse—Adaptation of the sciatic static index. *Journal of Neuroscience Methods,* 161**,** 259-264.

BROCKES, J. P., FIELDS, K. L. & RAFF, M. C. 1979. Studies on cultured rat Schwann cells. I. Establishment of purified populations from cultures of peripheral nerve. *Brain Research,* 165**,** 105-118.

CIMADAMORE, F., AMADOR-ARJONA, A., CHEN, C., HUANG, C. T. & TERSKIKH, A. V. 2013. SOX2-LIN28/let-7 pathway regulates proliferation and neurogenesis in neural precursors. *Proc Natl Acad Sci U S A,* 110**,** E3017-26.

CRAWFORD, A. T., DESAI, D., GOKINA, P., BASAK, S. & KIM, H. A. 2008. E-cadherin expression in postnatal Schwann cells is regulated by the cAMP-dependent protein kinase a pathway. *Glia,* 56**,** 1637-47.

D'ANTONIO, M., MUSNER, N., SCAPIN, C., UNGARO, D., DEL CARRO, U., RON, D., FELTRI, M. L. & WRABETZ, L. 2013. Resetting translational homeostasis restores myelination in Charcot-Marie-Tooth disease type 1B mice. *J Exp Med,* 210**,** 821-38.

DESMAZIERES, A., DECKER, L., VALLAT, J. M., CHARNAY, P. & GILARDI-HEBENSTREIT, P. 2008. Disruption of Krox20-Nab interaction in the mouse leads to peripheral neuropathy with biphasic evolution. *J Neurosci,* 28**,** 5891-900.

DODDRELL, R. D., DUN, X. P., SHIVANE, A., FELTRI, M. L., WRABETZ, L., WEGNER, M., SOCK, E., HANEMANN, C. O. & PARKINSON, D. B. 2013a. Loss of SOX10 function contributes to the phenotype of human Merlin-null schwannoma cells. *Brain,* 136**,** 549-63.

DODDRELL, R. D. S., DUN, X.-P., MOATE, R. M., JESSEN, K. R., MIRSKY, R. & PARKINSON, D. B. 2012. Regulation of Schwann cell differentiation and proliferation by the Pax-3 transcription factor. *Glia,* 60**,** 1269-1278.

DODDRELL, R. D. S., DUN, X. P., SHIVANE, A., FELTRI, M. L., WRABETZ, L., WEGNER, M., SOCK, E., HANEMANN, C. O. & PARKINSON, D. B. 2013b. Loss of SOX10 function contributes to the phenotype of human Merlin-null schwannoma cells. *Brain,* 136**,** 549-63.

DUN, X. P. & PARKINSON, D. B. 2015. Visualizing peripheral nerve regeneration by whole mount staining. *PLoS One,* 10**,** e0119168.

FELTRI, M. L., D'ANTONIO, M., PREVITALI, S., FASOLINI, M., MESSING, A. & WRABETZ, L. 1999. P0-Cre transgenic mice for inactivation of adhesion molecules in Schwann cells. *Ann N Y Acad Sci,* 883**,** 116-23.

FERN, R., DAVIS, P., WAXMAN, S. G. & RANSOM, B. R. 1998. *Axon Conduction and Survival in CNS White Matter During Energy Deprivation: A Developmental Study*.

FINZSCH, M., SCHREINER, S., KICHKO, T., REEH, P., TAMM, E. R., BOSL, M. R., MEIJER, D. & WEGNER, M. 2010. Sox10 is required for Schwann cell identity and progression beyond the immature Schwann cell stage. *J Cell Biol,* 189**,** 701-12.

FONTANA, X., HRISTOVA, M., DA COSTA, C., PATODIA, S., THEI, L., MAKWANA, M., SPENCER-DENE, B., LATOUCHE, M., MIRSKY, R., JESSEN, K. R., KLEIN, R., RAIVICH, G. & BEHRENS, A. 2012. c-Jun in Schwann cells promotes axonal regeneration and motoneuron survival via paracrine signaling. *J Cell Biol,* 198**,** 127-41.

FROB, F., BREMER, M., FINZSCH, M., KICHKO, T., REEH, P., TAMM, E. R., CHARNAY, P. & WEGNER, M. 2012. Establishment of myelinating Schwann cells and barrier integrity between central and peripheral nervous systems depend on Sox10. *Glia,* 60**,** 806-19.

FUNALOT, B., TOPILKO, P., ARROYO, M. A., SEFIANI, A., HEDLEY-WHYTE, E. T., YOLDI, M. E., RICHARD, L., TOURAILLE, E., LAURICHESSE, M., KHALIFA, E., CHAUZEIX, J., OUEDRAOGO, A., CROS, D., MAGDELAINE, C., STURTZ, F. G., URTIZBEREA, J. A., CHARNAY, P., BRAGADO, F. G. & VALLAT, J. M. 2012. Homozygous deletion of an EGR2 enhancer in congenital amyelinating neuropathy. *Ann Neurol,* 71**,** 719-23.

GESS, B., HALFTER, H., KLEFFNER, I., MONJE, P., ATHAUDA, G., WOOD, P. M., YOUNG, P. & WANNER, I. B. 2008. Inhibition of N-cadherin and beta-catenin function reduces axon-induced Schwann cell proliferation. *J Neurosci Res,* 86**,** 797-812.

GIAMBONINI-BRUGNOLI, G., BUCHSTALLER, J., SOMMER, L., SUTER, U. & MANTEI, N. 2005. Distinct disease mechanisms in peripheral neuropathies due to altered peripheral myelin protein 22 gene dosage or a Pmp22 point mutation. *Neurobiol Dis,* 18**,** 656-68.

GILLESPIE, C. S., SHERMAN, D. L., BLAIR, G. E. & BROPHY, P. J. 1994. Periaxin, a novel protein of myelinating schwann cells with a possible role in axonal ensheathment. *Neuron,* 12**,** 497-508.

GOKBUGET, D., PEREIRA, J. A., BACHOFNER, S., MARCHAIS, A., CIAUDO, C., STOFFEL, M., SCHULTE, J. H. & SUTER, U. 2015. The Lin28/let-7 axis is critical for myelination in the peripheral nervous system. *Nat Commun,* 6**,** 8584.

GOLAN, N., KARTVELISHVILY, E., SPIEGEL, I., SALOMON, D., SABANAY, H., RECHAV, K., VAINSHTEIN, A., FRECHTER, S., MAIK-RACHLINE, G., ESHED-EISENBACH, Y., MOMOI, T. & PELES, E. 2013. Genetic deletion of Cadm4 results in myelin abnormalities resembling Charcot-Marie-Tooth neuropathy. *J Neurosci,* 33**,** 10950-61.

HANTKE, J., CARTY, L., WAGSTAFF, L. J., TURMAINE, M., WILTON, D. K., QUINTES, S., KOLTZENBURG, M., BAAS, F., MIRSKY, R. & JESSEN, K. R. 2014. c-Jun activation in Schwann cells protects against loss of sensory axons in inherited neuropathy. *Brain,* 137**,** 2922-37.

HARRISINGH, M. C., PEREZ-NADALES, E., PARKINSON, D. B., MALCOLM, D. S., MUDGE, A. W. & LLOYD, A. C. 2004a. The Ras/Raf/ERK signalling pathway drives Schwann cell dedifferentiation. *EMBO J,* 23**,** 3061-71.

HARRISINGH, M. C., PEREZ‐NADALES, E., PARKINSON, D. B., MALCOLM, D. S., MUDGE, A. W. & LLOYD, A. C. 2004b. *The Ras/Raf/ERK signalling pathway drives Schwann cell dedifferentiation*.

HUTTON, E. J., CARTY, L., LAURA, M., HOULDEN, H., LUNN, M. P., BRANDNER, S., MIRSKY, R., JESSEN, K. & REILLY, M. M. 2011. c-Jun expression in human neuropathies: a pilot study. *J Peripher Nerv Syst,* 16**,** 295-303.

ISHII, A., FURUSHO, M. & BANSAL, R. 2013. Sustained Activation of ERK1/2 MAPK in Oligodendrocytes and Schwann Cells Enhances Myelin Growth and Stimulates Oligodendrocyte Progenitor Expansion. *J Neurosci,* 33**,** 175-86.

ISHII, A., FURUSHO, M., DUPREE, J. L. & BANSAL, R. 2016. Strength of ERK1/2 MAPK Activation Determines Its Effect on Myelin and Axonal Integrity in the Adult CNS. *J Neurosci,* 36**,** 6471-87.

JAEGLE, M., MANDEMAKERS, W., BROOS, L., ZWART, R., KARIS, A., VISSER, P., GROSVELD, F. & MEIJER, D. 1996. The POU factor Oct-6 and Schwann cell differentiation. *Science,* 273**,** 507-10.

JESSEN, K. R., BRENNAN, A., MORGAN, L., MIRSKY, R., KENT, A., HASHIMOTO, Y. & GAVRILOVIC, J. 1994. The Schwann cell precursor and its fate: a study of cell death and differentiation during gliogenesis in rat embryonic nerves. *Neuron,* 12**,** 509-27.

JESSEN, K. R. & MIRSKY, R. 2008. Negative regulation of myelination: relevance for development, injury, and demyelinating disease. *Glia,* 56**,** 1552-65.

JESSEN, K. R. & MIRSKY, R. 2016. The repair Schwann cell and its function in regenerating nerves. *J Physiol*.

KAO, S. C., WU, H., XIE, J., CHANG, C. P., RANISH, J. A., GRAEF, I. A. & CRABTREE, G. R. 2009. Calcineurin/NFAT signaling is required for neuregulin-regulated Schwann cell differentiation. *Science,* 323**,** 651-4.

KIM, H. A., POMEROY, S. L., WHORISKEY, W., PAWLITZKY, I., BENOWITZ, L. I., SICINSKI, P., STILES, C. D. & ROBERTS, T. M. 2000. A developmentally regulated switch directs regenerative growth of Schwann cells through cyclin D1. *Neuron,* 26**,** 405-16.

KLEIN, D., GROH, J., WETTMARSHAUSEN, J. & MARTINI, R. 2014. Nonuniform molecular features of myelinating Schwann cells in models for CMT1: distinct disease patterns are associated with NCAM and c-Jun upregulation. *Glia,* 62**,** 736-50.

KUHN, P. L., PETROULAKIS, E., ZAZANIS, G. A. & MCKINNON, R. D. 1995. Motor function analysis of myelin mutant mice using a rotarod. *International Journal of Developmental Neuroscience,* 13**,** 715-722.

LE, N., NAGARAJAN, R., WANG, J. Y., ARAKI, T., SCHMIDT, R. E. & MILBRANDT, J. 2005a. Analysis of congenital hypomyelinating Egr2Lo/Lo nerves identifies Sox2 as an inhibitor of Schwann cell differentiation and myelination. *Proc Natl Acad Sci U S A,* 102**,** 2596-601.

LE, N., NAGARAJAN, R., WANG, J. Y. T., ARAKI, T., SCHMIDT, R. E. & MILBRANDT, J. 2005b. Analysis of congenital hypomyelinating Egr2Lo/Lo nerves identifies Sox2 as an inhibitor of Schwann cell differentiation and myelination. *Proceedings of the National Academy of Sciences of the United States of America,* 102**,** 2596-2601.

LEWALLEN, K. A., SHEN, Y. A., DE LA TORRE, A. R., NG, B. K., MEIJER, D. & CHAN, J. R. 2011. Assessing the role of the cadherin/catenin complex at the Schwann cell-axon interface and in the initiation of myelination. *J Neurosci,* 31**,** 3032-43.

LU, Y., FUTTNER, C., ROCK, J. R., XU, X., WHITWORTH, W., HOGAN, B. L. & ONAITIS, M. W. 2010. Evidence that SOX2 overexpression is oncogenic in the lung. *PLoS One,* 5**,** e11022.

MARSON, A., LEVINE, S. S., COLE, M. F., FRAMPTON, G. M., BRAMBRINK, T., JOHNSTONE, S., GUENTHER, M. G., JOHNSTON, W. K., WERNIG, M., NEWMAN, J., CALABRESE, J. M., DENNIS, L. M., VOLKERT, T. L., GUPTA, S., LOVE, J., HANNETT, N., SHARP, P. A., BARTEL, D. P., JAENISCH, R. & YOUNG, R. A. 2008. Connecting microRNA genes to the core transcriptional regulatory circuitry of embryonic stem cells. *Cell,* 134**,** 521-33.

MAUREL, P., EINHEBER, S., GALINSKA, J., THAKER, P., LAM, I., RUBIN, M. B., SCHERER, S. S., MURAKAMI, Y., GUTMANN, D. H. & SALZER, J. L. 2007. Nectin-like proteins mediate axon Schwann cell interactions along the internode and are essential for myelination. *J Cell Biol,* 178**,** 861-74.

MINDOS, T., DUN, X. P., NORTH, K., DODDRELL, R. D., SCHULZ, A., EDWARDS, P., RUSSELL, J., GRAY, B., ROBERTS, S. L., SHIVANE, A., MORTIMER, G., PIRIE, M., ZHANG, N., PAN, D., MORRISON, H. & PARKINSON, D. B. 2017. Merlin controls the repair capacity of Schwann cells after injury by regulating Hippo/YAP activity. *J Cell Biol,* 216**,** 495-510.

NAGARAJAN, R., SVAREN, J., LE, N., ARAKI, T., WATSON, M. & MILBRANDT, J. 2001. EGR2 Mutations in Inherited Neuropathies Dominant-Negatively Inhibit Myelin Gene Expression. *Neuron,* 30**,** 355-368.

NAPOLI, I., NOON, L. A., RIBEIRO, S., KERAI, A. P., PARRINELLO, S., ROSENBERG, L. H., COLLINS, M. J., HARRISINGH, M. C., WHITE, I. J., WOODHOO, A. & LLOYD, A. C. 2012. A central role for the ERK-signaling pathway in controlling Schwann cell plasticity and peripheral nerve regeneration in vivo. *Neuron,* 73**,** 729-42.

PARKINSON, D. B., BHASKARAN, A., ARTHUR-FARRAJ, P., NOON, L. A., WOODHOO, A., LLOYD, A. C., FELTRI, M. L., WRABETZ, L., BEHRENS, A., MIRSKY, R. & JESSEN, K. R. 2008a. c-Jun is a negative regulator of myelination. *J Cell Biol,* 181**,** 625-37.

PARKINSON, D. B., BHASKARAN, A., ARTHUR-FARRAJ, P., NOON, L. A., WOODHOO, A., LLOYD, A. C., FELTRI, M. L., WRABETZ, L., BEHRENS, A., MIRSKY, R. & JESSEN, K. R. 2008b. c-Jun is a negative regulator of myelination. *The Journal of Cell Biology,* 181**,** 625-637.

PARKINSON, D. B., BHASKARAN, A., DROGGITI, A., DICKINSON, S., D'ANTONIO, M., MIRSKY, R. & JESSEN, K. R. 2004a. Krox-20 inhibits Jun-NH2-terminal kinase/c-Jun to control Schwann cell proliferation and death. *The Journal of Cell Biology,* 164**,** 385-394.

PARKINSON, D. B., BHASKARAN, A., DROGGITI, A., DICKINSON, S., D'ANTONIO, M., MIRSKY, R. & JESSEN, K. R. 2004b. Krox-20 inhibits Jun-NH2-terminal kinase/c-Jun to control Schwann cell proliferation and death. *J Cell Biol,* 164**,** 385-94.

PARKINSON, D. B., DICKINSON, S., BHASKARAN, A., KINSELLA, M. T., BROPHY, P. J., SHERMAN, D. L., SHARGHI-NAMINI, S., DURAN ALONSO, M. B., MIRSKY, R. & JESSEN, K. R. 2003a. Regulation of the myelin gene periaxin provides evidence for Krox-20-independent myelin-related signalling in Schwann cells. *Molecular and Cellular Neuroscience,* 23**,** 13-27.

PARKINSON, D. B., DICKINSON, S., BHASKARAN, A., KINSELLA, M. T., BROPHY, P. J., SHERMAN, D. L., SHARGHI-NAMINI, S., DURAN ALONSO, M. B., MIRSKY, R. & JESSEN, K. R. 2003b. Regulation of the myelin gene periaxin provides evidence for Krox-20-independent myelin-related signalling in Schwann cells. *Mol Cell Neurosci,* 23**,** 13-27.

PARKINSON, D. B., DONG, Z., BUNTING, H., WHITFIELD, J., MEIER, C., MARIE, H., MIRSKY, R. & JESSEN, K. R. 2001. Transforming Growth Factor β (TGFβ) Mediates Schwann Cell Death In Vitro and In Vivo: Examination of c-Jun Activation, Interactions with Survival Signals, and the Relationship of TGFβ-Mediated Death to Schwann Cell Differentiation. *The Journal of Neuroscience,* 21**,** 8572-8585.

PARRINELLO, S., NAPOLI, I., RIBEIRO, S., DIGBY, P. W., FEDOROVA, M., PARKINSON, D. B., DODDRELL, R. D. S., NAKAYAMA, M., ADAMS, R. H. & LLOYD, A. C. 2010a. EphB Signaling Directs Peripheral Nerve Regeneration through Sox2-Dependent Schwann Cell Sorting. *Cell,* 143**,** 145-155.

PARRINELLO, S., NAPOLI, I., RIBEIRO, S., WINGFIELD DIGBY, P., FEDOROVA, M., PARKINSON, D. B., DODDRELL, R. D., NAKAYAMA, M., ADAMS, R. H. & LLOYD, A. C. 2010b. EphB signaling directs peripheral nerve regeneration through Sox2-dependent Schwann cell sorting. *Cell,* 143**,** 145-55.

ROBERTS, S. L., DUN, X. P., DEE, G., GRAY, B., MINDOS, T. & PARKINSON, D. B. 2016. The role of p38alpha in Schwann cells in regulating peripheral nerve myelination and repair. *J Neurochem*.

SAPORTA, M. A., SHY, B. R., PATZKO, A., BAI, Y., PENNUTO, M., FERRI, C., TINELLI, E., SAVERI, P., KIRSCHNER, D., CROWTHER, M., SOUTHWOOD, C., WU, X., GOW, A., FELTRI, M. L.,

WRABETZ, L. & SHY, M. E. 2012a. MpzR98C arrests Schwann cell development in a mouse model of early-onset Charcot-Marie-Tooth disease type 1B. *Brain,* 135**,** 2032-47.

SAPORTA, M. A. C., SHY, B. R., PATZKO, A., BAI, Y., PENNUTO, M., FERRI, C., TINELLI, E., SAVERI, P., KIRSCHNER, D., CROWTHER, M., SOUTHWOOD, C., WU, X., GOW, A., FELTRI, M. L., WRABETZ, L. & SHY, M. E. 2012b. *MpzR98C arrests Schwann cell development in a mouse model of early-onset Charcot–Marie–Tooth disease type 1B*.

SPIEGEL, I., ADAMSKY, K., ESHED, Y., MILO, R., SABANAY, H., SARIG-NADIR, O., HORRESH, I., SCHERER, S. S., RASBAND, M. N. & PELES, E. 2007. A central role for Necl4 (SynCAM4) in Schwann cell-axon interaction and myelination. *Nat Neurosci,* 10**,** 861-9.

SVAREN, J. & MEIJER, D. 2008. The molecular machinery of myelin gene transcription in Schwann cells. *Glia,* 56**,** 1541-51.

TOPILKO, P., SCHNEIDER-MAUNOURY, S., LEVI, G., BARON-VAN EVERCOOREN, A., CHENNOUFI, A. B., SEITANIDOU, T., BABINET, C. & CHARNAY, P. 1994. Krox-20 controls myelination in the peripheral nervous system. *Nature,* 371**,** 796-9.

TRUETT, G. E., HEEGER, P., MYNATT, R. L., TRUETT, A. A., WALKER, J. A. & WARMAN, M. L. 2000. Preparation of PCR-quality mouse genomic DNA with hot sodium hydroxide and tris (HotSHOT). *Biotechniques,* 29**,** 52, 54.

WANNER, I. B., GUERRA, N. K., MAHONEY, J., KUMAR, A., WOOD, P. M., MIRSKY, R. & JESSEN, K. R. 2006. Role of N-cadherin in Schwann cell precursors of growing nerves. *Glia,* 54**,** 439-59.

WANNER, I. B. & WOOD, P. M. 2002. N-cadherin mediates axon-aligned process growth and cell-cell interaction in rat Schwann cells. *J Neurosci,* 22**,** 4066-79.

WARNER, L. E., MANCIAS, P., BUTLER, I. J., MCDONALD, C. M., KEPPEN, L., KOOB, K. G. & LUPSKI, J. R. 1998. Mutations in the early growth response 2 (EGR2) gene are associated with hereditary myelinopathies. *Nat Genet,* 18**,** 382-4.

WARNER, L. E., SVAREN, J., MILBRANDT, J. & LUPSKI, J. R. 1999. Functional consequences of mutations in the early growth response 2 gene (EGR2) correlate with severity of human myelinopathies. *Hum Mol Genet,* 8**,** 1245-51.

WOODHOO, A., ALONSO, M. B., DROGGITI, A., TURMAINE, M., D'ANTONIO, M., PARKINSON, D. B., WILTON, D. K., AL-SHAWI, R., SIMONS, P., SHEN, J., GUILLEMOT, F., RADTKE, F., MEIJER, D., FELTRI, M. L., WRABETZ, L., MIRSKY, R. & JESSEN, K. R. 2009a. Notch controls embryonic Schwann cell differentiation, postnatal myelination and adult plasticity. *Nat Neurosci,* 12**,** 839-47.

WOODHOO, A., ALONSO, M. B. D., DROGGITI, A., TURMAINE, M., D'ANTONIO, M., PARKINSON, D. B., WILTON, D. K., AL-SHAWI, R., SIMONS, P., SHEN, J., GUILLEMOT, F., RADTKE, F., MEIJER, D., FELTRI, M. L., WRABETZ, L., MIRSKY, R. & JESSEN, K. R. 2009b. Notch controls embryonic Schwann cell differentiation, postnatal myelination and adult plasticity. *Nat Neurosci,* 12**,** 839-847.

WRABETZ, L., D'ANTONIO, M., PENNUTO, M., DATI, G., TINELLI, E., FRATTA, P., PREVITALI, S., IMPERIALE, D., ZIELASEK, J., TOYKA, K., AVILA, R. L., KIRSCHNER, D. A., MESSING, A., FELTRI, M. L. & QUATTRINI, A. 2006. Different intracellular pathomechanisms produce diverse Myelin Protein Zero neuropathies in transgenic mice. *J Neurosci,* 26**,** 2358-68.

YANG, D. P., KIM, J., SYED, N., TUNG, Y. J., BHASKARAN, A., MINDOS, T., MIRSKY, R., JESSEN, K. R., MAUREL, P., PARKINSON, D. B. & KIM, H. A. 2012. p38 MAPK activation promotes denervated Schwann cell phenotype and functions as a negative regulator of Schwann cell differentiation and myelination. *J Neurosci,* 32**,** 7158-68.